Biochimica et Biophysica Acta 1837 (2014) 783–791

Contents lists available at ScienceDirect

Biochimica et Biophysica Acta

journal homepage: www.elsevier.com/locate/bbabio

Epigallocatechin gallate counteracts oxidative stress in docosahexaenoxic acid-treated myocytes

Ester Casanova, Laura Baselga-Escudero, Aleix Ribas-Latre, Anna Arola-Arnal, Cinta Bladé, Lluís Arola, M. Josepa Salvadó *

Grup de Nutrigenòmica, Departament de Bioquimica i Biotecnologia, Universitat Rovira i Virgili, Campus Sescel·lades, 43007 Tarragona, Spain

ARTICLE INFO

Article history:
Received 6 November 2013
Received in revised form 17 January 2014
Accepted 23 January 2014
Available online 28 January 2014

Keywords:
Docosahexaenoic acid
Epigallocatechin gallate
Skeletal muscle
Mitochondria
Reactive oxygen species
Antioxidant

ABSTRACT

Skeletal muscle is a key organ of mammalian energy metabolism, and its mitochondria are multifunction organelles that are targets of dietary bioactive compounds. The goal of this work was to examine the regulation of mitochondrial dynamics, functionality and cell energy parameters using docosahexaenoic acid (DHA), epigallocatechin gallate (EGCG) and a combination of both in L6 myocytes. Compounds (at 25 μM) were incubated for 4 h. Cells cultured with DHA displayed less oxygen consumption with higher ADP/ATP ratio levels concomitant with downregulation of *Cox* and *Ant1* gene expression. The disruption of energetic homeostasis by DHA, increases intracellular reactive oxygen species (ROS) levels and decreases mitochondrial membrane potential. The defence mechanism to counteract the excess of ROS production was by the upregulation of *Ucp2*, *Ucp3* and *MnSod* gene expression. Moreover myocytes cultured with DHA had a higher mitochondrial mass with a higher proportion of large and elongated mitochondria, whereas the fission genes *Drp1* and *Fiss1* and the fusion gene *Mfn2* were downregulated. In myocytes co-incubated with DHA and EGCG, ROS levels and the adenosine diphosphate (ADP)/adenosine triphosphate (ATP) ratio were similar to untreated myocytes and the decrease of oxygen consumption, higher mitochondrial mass and the overexpression of *Ucp2* and *Ucp3* genes were similar to the DHA-treated cells with also a higher amount of mitochondrial deoxyribonucleic acid (DNA), and reduced *Drp1* and *Fiss1* gene expression levels. In conclusion the addition of EGCG to DHA returned the cells to the control conditions in terms of mitochondrial morphology, energy and redox status, which were unbalanced in the DHA-treated myocytes.

1. Introduction

Mitochondria are ubiquitous organelles in eukaryotic cells whose primary functions are to generate energy, regulate the cellular redox state and calcium homeostasis, and initiate cellular apoptosis [1]. In addition, mitochondria are the main intracellular source and immediate target of reactive oxygen species (ROS), which are continuously generated as byproducts of aerobic metabolism in mammalian cells. Thus, mitochondria play a pivotal role in the determination of the life and death of the mammalian cell [2]. The size, shape, and abundance of mitochondria vary dramatically in different cell types and may change under different energy demands and physiological environmental conditions [3]. In many cell types, especially muscle fibres, mitochondria form tubular structures or networks [4]. Increasing evidence, suggests that mitochondrial structure determines mitochondrial function [5] including substrate metabolism and mitochondrial bioenergetics. Mitochondria are highly dynamic organelles with constant fusion and fission events mediated by conserved cellular machineries. The frequencies of these fusion and fission events are balanced to maintain the overall morphology of the mitochondrial population [6] and to control mitochondrial energy metabolism, protecting cells from mitochondrial damage and maintain the overall architecture of these organelles [7,8].

Mitochondria are recognised as major targets of bioactive compounds, such as omega-3 polyunsaturated fatty acids (PUFAs) and flavonoids, which are found in healthy diets. The current data support a role for omega-3 PUFA supplementation, particularly docosahexaenoic acid (DHA), which is strongly associated with changes

Abbreviations: AFU, arbitrary fluorescence units; *Ant* 1, adenine nucleotide translocase 1; *Cox*, cytochrome c oxidase subunit V; *Cs*, citrate synthase; DCFH-DA, 2′,7′-dichlorofluorescin diacetate; DHA, docosahexaenoic acid; DMEM, Dulbecco's modified Eagle's medium; *Drp1*, dynamin-related protein 1; EGCG, epigallocatechin-3-gallate; ETC, electron transport chain; ETS, electron transport capacity; FBS, fetal bovine serum; FCCP, carbonyl cyanide 4-(trifluoromethoxy)phenylhydrazone; *Fiss1*, mitochondrial fission 1 protein; Fluo-3 AM, fluo-3 acetoxymethyl ester; *Gapdh*, glyceraldehydes-3-phosphate dehydrogenase; LDH, lactate dehydrogenase; *Mfn2*, mitofusin 2; MMP, mitochondrial membrane potential; *MnSod*, manganese superoxide dismutase; mtDNA, mitochondrial DNA; nDNA, nuclear DNA; *Nd3*, NADH-dehydrogenase subunit 3; OXPHOS, oxidative phosphorylation; *Opa1*, optic atrophy 1; PUFAs, polyunsaturated fatty acids; Rhd123, Rhodamine 123; ROS, reactive oxygen species; ROX, residual oxygen consumption; *Ucp2*, uncoupling protein 2; *Ucp3*, uncoupling protein 3

* Corresponding author at: Department of Biochemistry and Biotechnology, Universitat Rovira i Virgili, C/Marcel·lí i Domingo s/n, 43007 Tarragona, Spain. Tel.: +34 977559567; fax: +34 977558232.
E-mail address: mariajosepa.salvado@urv.cat (M.J. Salvadó).

0005-2728/$ – see front matter © 2014 Elsevier B.V. All rights reserved.
http://dx.doi.org/10.1016/j.bbabio.2014.01.014

and the remodelling of mitochondrial phospholipid composition and organisational domains [9–14]. Although DHA is a likely target for oxidation [15–17], its health benefits are largely derived through DHA (22:6n − 3) rapidly in place of other fatty acids into biological membranes, particularly plasma and mitochondrial membranes and its cell signalling mechanisms. Incorporation of 22:6n − 3 influences membrane structure and function [18], increasing membrane permeability [19] fluidity and plasticity altering conformational states with their acyl chains, which are extremely flexible [13], and influences the physical properties of biological membranes, thereby altering protein function and fusion [13,20]. In addition to being susceptible to lipid peroxidation, DHA could decrease mitochondrial function simply as a result of the accumulation of oxidised products [21], altering the lipid bilayer and decreasing bioenergetic activities due to membrane perturbations [19]. In mitochondria, PUFAs play a role in several mitochondrial processes, including mitochondrial calcium homeostasis, gene expression, and respiratory function, and act as protonophores to reduce mitochondrial ROS production through uncoupling protein (UCP)-mediated decreases in mitochondrial membrane potential [17].

Mitochondria can also be regarded as important intracellular targets of agents that protect from the undesirable action of ROS, such as polyphenols, which prevent against many pathological states involving oxidative cell damage [22]. Epigallocatechin-3-gallate (EGCG) is the most abundant polyphenol isolated from green tea and is widely studied because it promotes cardiovascular and metabolic health by acting as a potent antioxidant that may have therapeutic applications in the treatment of many disorders. EGCG has antioxidant properties [23–25] with powerful radical scavengers. These antioxidant activities are due to the presence of phenolic groups that are sensitive to oxidation and are increased by the presence of the trihydroxyl structure in the D ring of EGCG [26]. Therefore, the presence of antioxidants jointly with omega-3 PUFAs would prevent possible oxidative deterioration. Despite the beneficial response of EGCG and DHA in muscle cells, here, we tested the hypothesis that EGCG has protective effects on the DHA oxidation, associated to the changes of physical properties of biological membranes and consequent changes in energy metabolism due to DHA intake. Taking into account that skeletal muscle tissue is a major determinant of whole-body energy metabolism, the aim of this study was to examine how EGCG and DHA, alone or in combination, affect cell energy homeostasis, mitochondrial functionality and morphology, oxidative phosphorylation, ROS generation and calcium homeostasis in L6 myocytes.

2. Materials and methods

2.1. Chemicals

(−) Epigallocatechin-3-gallate (EGCG) from green tea, cis-4,7,10,13,16,19-docosahexaenoic acid (DHA), fatty acid-free BSA, 2′,7′-dichlorofluorescin diacetate (DCFH-DA), DMSO, Bradford reagent, carbonyl cyanide 4-(trifluoromethoxy)phenylhydrazone (FCCP), oligomycin, rotenone, antimycin A, rhodamine 123 (Rhd123), ethanol, succinate and Fluo-3 acetoxymethyl ester (Fluo-3 AM) were obtained from Sigma-Aldrich (Madrid, Spain), and the MitoTracker FM was obtained from Molecular Probes (Eugene, Oregon, USA). Dulbecco's modified Eagle's medium (DMEM), glutamine, fetal bovine serum (FBS), penicillin and streptomycin were obtained from BioWhittaker (Verviers, Belgium).

2.2. Cell culture

L6 myocyte cells (kindly supplied from Dr. Manuel Portero-Otín) were routinely cultivated in DMEM supplemented with 2 mM glutamine, 10% FBS, 1% penicillin (126.6 U/mL) and 1% streptomycin (0.126 mg/mL) at 37 °C in an atmosphere of 5% CO_2. The cells were grown to approximately 80% confluence and then induced to differentiate into myotubes in DMEM supplemented with 2% FBS. After 7 days, myotube differentiation was complete, and the experimental procedure was initiated. L6 cells were serum-starved for 4 h before the assay. All experiments were performed in triplicate in 3 independent experiments.

2.3. Cell treatment

To study the effects of EGCG, DHA and the combination of both compounds on mitochondrial function, metabolism and morphology, L6 myocyte cells were treated with the vehicle control, 25 μM EGCG, 25 μM DHA, or 25 μM EGCG + 25 μM DHA. Both compounds were dissolved in ethanol and added to the culture media. The medium used during the treatment was serum-free DMEM containing 2% BSA. The experiments were performed in triplicate and with 3 different passages. The final concentration of ethanol in the media was 0.05%, a nontoxic percentage. After 4 h, the cells were used for the different analyses.

2.4. Cell death

Cell death was assessed by lactate dehydrogenase (LDH) leakage into the culture medium. Following the 24 h of exposure to EGCG and DHA (25 μM), the culture medium was aspirated and centrifuged at 3000 rpm for 5 min to obtain a cell-free supernatant; on the other hand cells were lysed in cold buffer (25 mM HEPES pH 7.0, 0.1% Triton X-100). The next steps were performed according to the manufacturer's instructions for the LDH kit (QCA; Amposta, Spain). The % of LDH leakage was normalised to control group and calculated as follows:

$$\%\text{LDH leakage} = ((\text{mUmedium})/(\text{mU medium} * \text{mU cells})) * 100.$$

2.5. Oxygen consumption assay in intact cells

In vivo measurements of mitochondrial oxygen consumption with intact cells were performed using a high-resolution oxygraph (Oroboros Instruments, Innsbruck, Austria) to quantify the respiration states. L6 myocytes were treated in 6-well plates and removed from culture dishes through trypsinisation (0.05% trypsin–EDTA). After 5 min of centrifugation at 200 *g* (room temperature), the cells were resuspended in warmed respiration medium (DMEM without fetal bovine serum) and transferred to the corresponding respiration chamber at a concentration of 4–6 × 10^6 cells/mL. Analyses of respiration rates were performed in 2 mL of respiration medium at 37 °C with stirring at 750 rpm. When the oxygen concentration was stabilised, basal respiration was recorded (Routine state) to control the levels of respiration and phosphorylation in a physiologically coupled state, which was supported by exogenous substrates in the culture media. Following stabilisation of the Routine state, ATP synthesis was inhibited with 2 μg/mL oligomycin, and the nonphosphorylating or resting state (Leak state) was recorded. Subsequently, 10–12 μM FCCP was added to stimulate respiration maximally at a level flow, measuring the electron transport system (ETS) capacity in the noncoupled state (ETS state). In sum, respiration was blocked with 2.5 μM rotenone and 2.5 μM antimycin, representing the residual oxygen consumption (ROX) state that remains after electron transport chain (ETC) inhibition. The results are expressed as oxygen flow per number of cells (pmol oxygen/10^6 cells * s). All results were corrected using the ROX state capacity. Oxygen consumption was calculated using DataGraph Software from Oroboros Instruments (Innsbruck, Austria).

2.6. Determination of ADP/ATP ratio

The total ADP/ATP ratio in the muscle cells was determined after 4 h of treatment using the ApoSENSOR™ ADP/ATP ratio assay kit (Biovision, Mountain View, CA, USA) following the manufacturer's instructions.

2.7. Intracellular ROS generation

The levels of intracellular ROS were quantified using the fluorescent probe 2′,7′-dichlorofluorescein-diacetate (DCFH-DA) [27]. A stock solution (10 mM) of DCFH was prepared in DMSO. Cells (2×10^6 per well) were incubated in black 24-well plates with clear bottoms. DCFH-DA diffuses into cells and becomes trapped inside the cell after being cleaved by intracellular esterases.

After treatment, the cells were washed twice with warmed PBS, and 10 μM of DCFH diluted in PBS was then loaded into the wells for 30 min at 37 °C in the dark. The cells were then gently washed twice in PBS to remove the excess dye and resuspended in 0.5 mL of PBS per well. The fluorescence intensity was recorded over 4 h as a measure of the degree of cellular oxidative stress. Intracellular ROS production was measured using an FLx800 Multi-Detection Microplate Reader (BioTek, Winooski, USA) at an excitation wavelength of 485 nm and an emission wavelength of 530 nm (37 °C). The measured fluorescence values are expressed as a percentage of fluorescence with respect to the control group.

2.8. Measurement of mitochondrial membrane potential (MMP)

MMP was monitored using Rhd123 dye fluorescence with an excitation wavelength of 525 nm and an emission wavelength of 485 nm using an FLx800 Multi-Detection Microplate Reader (BioTek; Winooski, USA) at 37 °C. Rhd123 is a membrane-permeant cation that is strongly sequestered in mitochondria due to their negative membrane potential. If mitochondria become depolarised, Rhd 123 is redistributed from the mitochondria to the cytosol, where it becomes diluted and, as a consequence, the fluorescence increases. Therefore, a decrease in fluorescence corresponds to an increase in MMP. To perform the analysis, cells (2×10^6 per well) were incubated in black 24-well plates with clear bottoms. Rh123 was dissolved in ethanol as a 0.5 mM stock solution. After treatment, the cells were washed 3 times with warm PBS and permeated with a permeating solution (0.5 μg/mL digitonin, 250 mM sucrose, 1 mM EDTA, 50 mM KCl, 2 mM KH_2PO_4, 25 mM Tris–HCl (pH 7.4)). To initiate the assay, 6 mM of succinate and 0.5 μg/mL Rhd 123 were added to the wells. Fluorescence was recorded after the addition of 2 μg/mL oligomycin to inhibit the ATP synthase, and 10 μg/mL of FCCP was then added to visualise the complete depolarisation. The results are expressed as a % compared to the control group.

2.9. Measurement of intracellular Ca^{2+} levels

Intracellular Ca^{2+} was measured using the fluorescent calcium indicator Fluo-3 AM. This dye is a fat-soluble reagent, is not fluorescent and is membrane permeate. Intracellular esterases break down the Fluo-3 AM ester into acetoxymethyl and Fluo-3, which can then combine with free intracellular calcium ions. The intensity of the fluorescence is dependent on the free calcium concentration. L6 cells were treated in 24-well black plates with clear bottoms. After treatment, the cells were washed three times in standard medium (141 mM NaCl, 4.7 mM KCl, 1.8 mM $CaCl_2$, 1.2 mM $MgSO_4$, 10 mM glucose, 10 mM HEPES (pH 7.4)). The cells were loaded with Fluo-3 AM (5 μM) for 45 min (37 °C) in the dark in the standard medium. The cells were then washed again to allow for the cleavage of the acetoxymethyl esters and resuspended in the standard medium or Ca^{2+}-free solution (the same as the standard medium except for the addition of calcium). Fluorescence was measured after 30 min using an FLx800 Multi-Detection Microplate Reader (Biotek, Winooski, USA) with an excitation wavelength of 503 and emission wavelength of 526 (37 °C). The Ca^{2+} level is expressed as a percentage of the fluorescence intensity relative to the control group's fluorescence intensity.

2.10. RNA extraction and quantitative real-time PCR (qRT-PCR) analysis

Total RNA was obtained from L6 cells using a RNeasy Mini kit (Qiagen; Valencia, Spain) according to the manufacturer's protocol. RNA (4 μg) was reverse transcribed to complementary DNA from the total RNA using a reverse transcription reagent kit (Applied Biosystems; Madrid, Spain). Gene expression was analysed by qRT-PCR amplification using TaqMan Universal 2× PCR Master Mix (Applied Biosystems; Madrid, Spain) and a PCR 7300 system (Applied Biosystems; Madrid, Spain) according to the manufacturer's instructions.

The thermal cycling consisted of an initial step at 50 °C for 2 min, followed by a polymerase activation step at 95 °C for 10 min and a cycling step with the following conditions: 40 cycles of denaturation at 95 °C for 15 s and annealing at 60 °C for 1 min. Specific TaqMan assay-on-demand probes were used to amplify the cDNA: cyclophilin peptidylprolyl isomerase A (*Ppia*) (Rn00690933_m1) (used as an endogenous control gene), cytochrome *c* oxidase subunit V (*Cox*) (Rn 00821806_m1), citrate synthase (*Cs*) (Rn00756225_m1), ATP5A1 (*ATPase*) (Rn01527025_m1), adenine nucleotide translocase 1 (*Ant1*) (Rn 00821477_g1), uncoupling protein 3 (*Ucp3*) (Rn00565874_m1), uncoupling protein 2 (*Ucp2*) (Rn00571166_m1), manganese superoxide dismutase (*MnSod*) (Rn00566942_g1), mitochondrial fission 1 protein (*Fiss1*) (Rn01480911_m1), dynamin-related protein 1 (*Drp1*) (Rn00586466_m1), mitofusin 2, (*Mfn2*) (Rn00500120_m1), and optic atrophy 1 (Rn_00592200_m1) (*Opa1*). The expression levels were normalised to cyclophilin using a comparative ($2^{-\Delta\Delta Ct}$) method.

2.11. Measurement of mtDNA/nDNA ratio

Total DNA was extracted from cells using a Qiamp DNA mini kit (Qiagen; Valencia, Spain) according to the manufacturer's instructions. The relative mitochondrial DNA (mtDNA) levels were measured by real-time PCR using the PCR 7300 system (Applied Biosystems, Madrid, Spain) and normalised by simultaneous measurement of the nuclear DNA (nDNA), (mtDNA/nDNA ratio). Primers and probes for quantitative PCR (qPCR) were designed using Primer Express (Applied Biosystems, Madrid, Spain): *Nd3* mitochondrial gene (forward: 5′-cttatcttttatcctcatttcaattgca-3′, reverse: 5′-gtagtgggtattggttgtttgaatc gctc-3′) and *Gapdh* as a nuclear gene (forward: 5′-ccagaacatcatccctg cat-3′; reverse: 5′-gttcagctctgggatgacctt-3′).

PCR conditions were 95 °C for 15 min, followed by 40 cycles of 95 °C for 15 s, and 60 °C for 60 s. The threshold cycle number (Ct) values for mitochondrial NADH-dehydrogenase subunit 3 (*Nd3*) and glyceraldehydes-3-phosphate dehydrogenase (*Gapdh*) were determined. The results were calculated from the difference in threshold cycle (ΔC_t) values for mtDNA and nuclear-specific amplification.

2.12. Measurement of mitochondrial morphology

To determine the mitochondrial morphology of individual cells, L6 myocytes were grown on coverslips inside 6-well collagen-treated plates filled with the appropriate culture medium. After treatment, the media was removed from the dish, and the cells were washed 3 times with prewarmed PBS. The cells were stained and incubated at 37 °C for 30 min with 400 nM MitoTracker Green FM. After staining cells were washed twice in PBS. The solution was then replaced with fresh media, and the cells were coverslipped for fluorescence microscopy to examine their morphology. Confocal images were obtained using a confocal laser-scanning microscope (NIKON TE-2000; Tokyo, Japan) with a 60× objective. MitoTracker Green FM preferentially accumulates in mitochondria regardless of the mitochondrial membrane potential and provides an accurate assessment of mitochondrial mass. For the quantification of mitochondrial morphology, mitochondrial length was measured and grouped into three categories as follows: short type (1 μm ≤ in length), medium rod type (1–2 μm in length) and long

type (>2 μm) using Image J software. Results are shown as a percentage of the total number mitochondria counted per treatment.

2.13. Statistical analyses

The results are expressed as the mean ± SEM of 6 animals. SPSS Statistics version 19 software (SPSS Inc., Chicago, IL, USA) was used for statistical analyses. Significant differences were analysed using one-way analysis of variance (ANOVA) followed by Tukey's post-hoc test. A p-value ≤ 0.05 was considered statistically significant.

3. Results

3.1. DHA increases the ADP/ATP ratio in addition to lowering oxygen consumption in intact L6 cells even when combined with EGCG

Cell death did not change when cells were treated with the selected physiological concentration of 25 μM for EGCG and DHA, as assessed by % LDH leakage (Fig. 1). Fig. 2 presents the changes in respiration caused by the different treatments in Routine, Leak and ETS states. The Routine state (Fig. 2a) controls physiological respiration through the cellular energy demand and is supported by the substrates in the culture media. Here, in the Routine state, despite neither EGCG nor DHA modified cell viability, treatment with DHA or DHA + EGCG for 4 h significantly reduced the oxygen consumption of the L6 cells, whereas there were no significant differences in oxygen consumption between the EGCG and control groups. By measuring the respiration rate in the presence of oligomycin, an ATPase inhibitor that is a direct measure of uncoupled respiration (Leak state) *in situ* (Fig. 2b), it has been shown that in the DHA and EGCG + DHA groups, oxygen consumption was significantly decreased. In addition in the ETS state (Fig. 2c), in the presence of FCCP, an uncoupler to measure the maximal respiratory capacity, a decrease in the DHA and EGCG + DHA groups compared to the control and EGCG groups was evident, though not statistically significant.

Fig. 2d presents a representative trace for the oxygen concentration in the chamber. This chart shows the differences between the groups in terms of the oxygen consumed in the different states and dependent on the treatment used. It clearly indicates that the DHA group tends to consume less oxygen during all recording states, especially in ETS states.

Moreover, the ADP/ATP ratio (Fig. 3) that refers to the energy status of cells was significantly higher in the DHA group and significantly lower in the EGCG group, whereas in the EGCG + DHA group, the ADP/ATP ratio was similar to that of the control group.

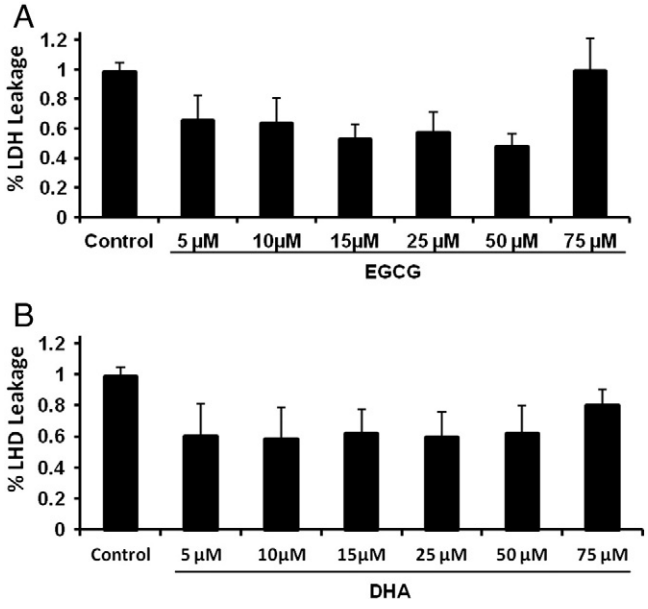

Fig. 1. % LDH leakage of L6 cells under different concentrations of EGCG and DHA. Cells were incubated with increasing concentrations (5 μM, 10 μM, 15 μM, 25 μM, 50 μM, 75 μM) of epigallocatechin-3-gallate (EGCG) or docosahexaenoic acid (DHA) for 24 h and cell death was assessed by the lactate dehydrogenase (LDH) method. The results are expressed in % LDH Leakage normalised to the control group and represent the mean ± SEM of triplicate measurements and are representative of three independent experiments. Different letters indicate statistical significance ($p \leq 0.05$).

3.2. EGCG reverses the increase of intracellular ROS caused by DHA treatment

The treatment with 25 μM DHA for 4 h significantly increased (150%) the intracellular ROS levels (Fig. 4) compared to the control and EGCG groups. In contrast, treatment with 25 μM DHA concomitant with 25 μM EGCG attenuated and reversed the increase in ROS levels induced by DHA.

3.3. DHA downregulates genes related to mitochondrial function, upregulates MnSod in parallels with Ucps, which maintained upregulation with EGCG cotreatment

The effects of DHA, EGCG and DHA + EGCG on the mRNA gene expression of marker enzymes of mitochondrial functionality are shown in Table 1. As in the respiration analyses, treatment with 25 μM EGCG did not induce a change in mitochondrial gene expression. In the case of 25 μM DHA treatment, *Cs* and *ATPase* gene expression did not differ between the groups. In contrast, *Cox* and *Ant1* gene expression were downregulated compared to the control group; however, *Cox* and *Ant1* were not downregulated when the cells were treated with DHA concomitant with EGCG. Both uncoupling protein genes (*Ucp2* and *Ucp3*) are expressed in muscle cells and were significantly upregulated in the DHA and EGCG + DHA groups. In examining the antioxidant system of the mitochondria, *MnSod* gene expression was significantly upregulated by DHA treatment compared to the control, but not in the co-treatment group.

3.4. DHA decreases mitochondrial membrane potential simultaneously with an increase of intracellular Ca^{2+} levels

Fig. 5 shows the results for the MMP measurements, there was a significant increase in arbitrary fluorescence unit (AFU) values for the DHA treatment with respect to the control conditions, indicating a decrease in the membrane potential. On the other hand intracellular calcium was elevated in DHA treatment with the presence of Ca^{2+} in the medium (Fig. 6a). This elevation was not produced when a Ca^{2+}-free solution was used (Fig. 6b).

3.5. DHA and EGCG + DHA increase mtDNA and downregulate enzymes involved in mitochondrial dynamics

Dynamin-related GTPases mediate the fission and fusion of mitochondrial membranes. In the outer membrane, *Mfn1*and *Mfn2*, are involved in the dynamic formation of the mitochondrial network. Similarly, *Opa1*, which is in the inner membrane, controls mitochondrial membrane fusion, whereas *Drp1* and *Fiss1* trigger fission events [28].

The results of how EGCG and/or DHA compounds modulated the expression of genes implicated in mitochondrial dynamics are shown in Table 2.

The mRNA contents of both *Fiss1* and *Drp1* were reduced in response to DHA and EGCG + DHA compounds, thus DHA treatment seems to prevent mitochondrial fission.

Likewise, *Mfn2* that takes part in mitochondrial fusion was significantly downregulated with the DHA treatment compared to the control group; however, in terms of *Opa1* expression, there were no significant differences between the groups.

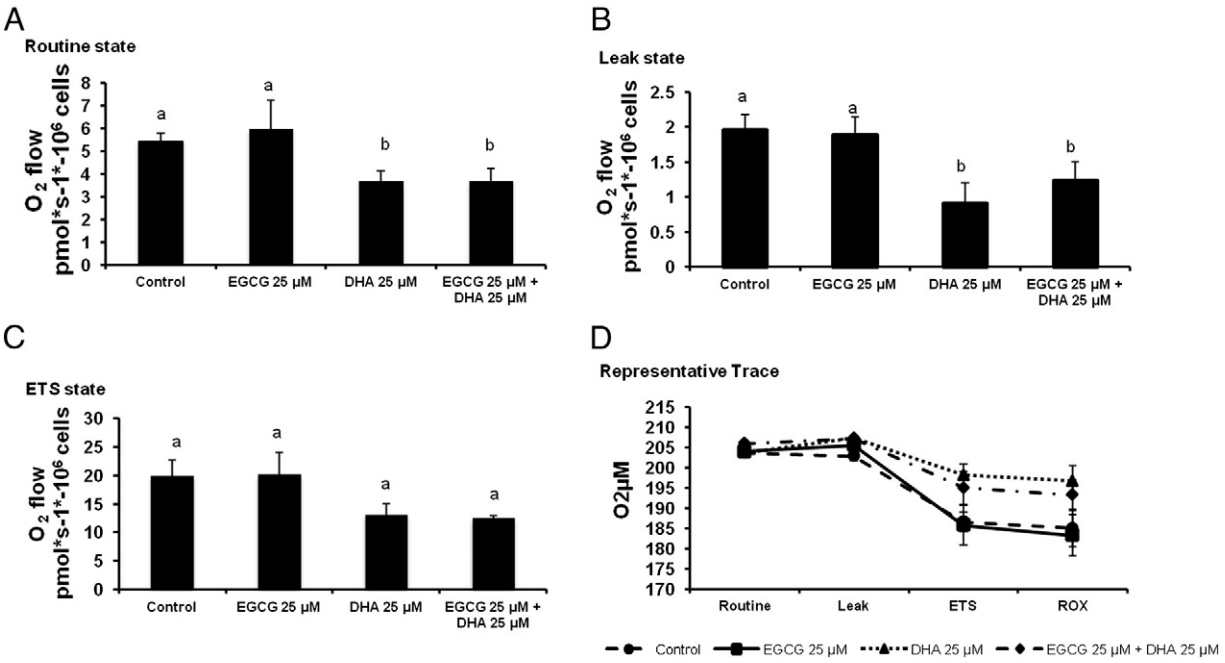

Fig. 2. Oxygen consumption of L6 cells under different treatments. Cells were incubated with 25 μM epigallocatechin-3-gallate (EGCG), docosahexaenoic acid (DHA) or EGCG + DHA for 4 h. *In vivo* oxygen consumption was then measured using high-resolution respirometry in different intact cell states: A. Routine state, B. Leak state, C. Electron transport system (ETS) capacity state. D. Oxygen consumption trace in the chamber in the different states: Routine, Leak, ETS and residual oxygen consumption (ROX). The results are expressed as the mean ± SEM of triplicate measurements and are representative of three independent experiments. Different letters indicate statistical significance ($p \leq 0.05$).

On the other hand, although the mRNA levels of fusion and fission gene expression are being downregulated by DHA, as shown in Fig. 7 the relative amount of mtDNA undergoes a significant 58% increase in the DHA-treated cells compared to the control group. Moreover, in the EGCG + DHA group, there was also an increase of approximately 61% compared with the control group.

3.6. Mitochondrial morphology after the DHA and EGCG treatments

To investigate whether EGCG and DHA directly alter mitochondrial dynamics, a morphological analysis was performed using fluorescence microscopy with the mitochondrial mass marker MitoTracker Green FM, which provided information about mitochondrial organisation and dynamics in L6 myocytes. Fig. 8a and e shows that the L6 control cells exhibited tubular networks with a higher proportion of round spheres, medium mitochondrial length and stubby mitochondria. After EGCG treatment (Fig. 8b and e), the mitochondrial morphology was similar to the control groups, with round spheres and medium length shapes. In contrast, the mitochondrial morphology after DHA treatment (Fig. 8c) was shifted toward a fragmented mitochondria with a discontinuous network and with a higher proportion of large and elongated mitochondria. Despite changes in mitochondrial visual morphology in DHA treatment there was an increase of medium mitochondria (Fig. 8e). Co-treatment with EGCG (Fig. 8d) and DHA reversed the mitochondrial fragmentation, restoring the mitochondrial network with an increase in elongated mitochondria, and rounder mitochondria with short and medium lengths (Fig. 8e).

4. Discussion

The beneficial effects of PUFAs against obesity and cardiovascular diseases have been well described [29,30]. Moreover polyphenols have also been demonstrated to exhibit a variety of beneficial biological properties, also including obesity and cardiovascular disease [31,32]. Especially DHA, as a normal component of the human diet could perform unusual shapes that could impact packing and hence membrane structure and properties that affect cellular function including signalling pathways, that may explain the wide variety of reported health benefits of n − 3 PUFAs [33]. But it is important to note that their structure with

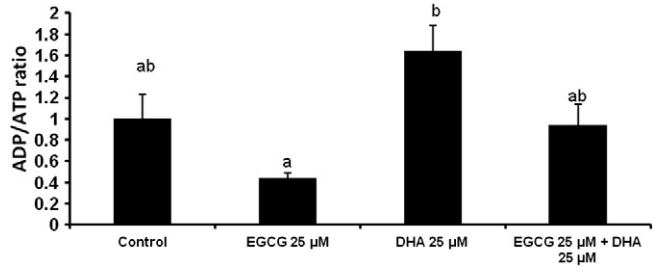

Fig. 3. ADP/ATP ratio in L6 cells treated with EGCG, DHA or DHA + EGCG. Cells were incubated with 25 μM epigallocatechin-3-gallate (EGCG), docosahexaenoic acid (DHA) or EGCG + DHA for 4 h. The ADP/ATP ratio was then measured using an Aposensor kit. The results are expressed as the mean ± SEM of triplicate measurements and are representative of three independent experiments. Different letters indicate statistically significant differences ($p \leq 0.05$) among the different groups.

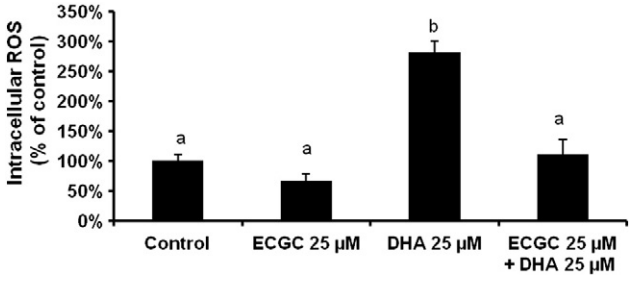

Fig. 4. ROS levels in L6 cells treated with EGCG, DHA or EGCG + DHA. Cells were incubated with 25 μM epigallocatechin-3-gallate (EGCG), docosahexaenoic acid (DHA) or EGCG + DHA for 4 h. Intracellular reactive oxygen species (ROS) was then measured using the fluorescent probe 2′,7′-dichlorofluorescein-diacetate (DCFH-DA) assay. The results are expressed as the mean ± SEM of triplicate measurements and are representative of three independent experiments. Different letters indicate statistically significant differences ($p \leq 0.05$) among the different groups.

Table 1
mRNA expression indicating mitochondrial function in L6 cells treated with DHA, EGCG or DHA + EGCG.

	Control	EGCG (25 μM)	DHA (25 μM)	EGCG + DHA (25 μM each)
Cox	1.00 ± 0.03a	0.99 ± 0.09ab	0.82 ± 0.03b	0.77 ± 0.08ab
Cs	1.00 ± 0.03a	0.92 ± 0.07a	1.02 ± 0.06a	0.92 ± 0.06a
ATPase	1.00 ± 0.02a	1.04 ± 0.03a	1.01 ± 0.05a	0.85 ± 0.08a
Ant1	1.00 ± 0.02a	0.89 ± 0.07ab	0.86 ± 0.03b	0.89 ± 0.04ab
Ucp3	1.23 ± 0.15a	1.32 ± 0.28a	2.51 ± 0.29b	2.03 ± 0.37b
Ucp2	1.05 ± 0.16a	1.29 ± 0.12a	2.48 ± 0.07b	2.11 ± 0.37b
MnSod	1.00 ± 0.05a	1.21 ± 0.16ab	1.18 ± 0.17b	1.13 ± 0.01ab

Cells were incubated with 25 μM epigallocatechin-3-gallate (EGCG), docosahexaenoic acid (DHA) or EGCG + DHA for 4 h. Different mRNA levels associated with the oxidative phosphorylation system (OXPHOS) such as cytochrome *c* oxidase subunit V (*Cox*), citrate synthase (*Cs*), ATP5A1 (*ATPase*), adenine nucleotide translocase 1 (*Ant1*), uncoupling protein 3 (*Ucp3*), uncoupling protein 2 (*Ucp2*), and manganese superoxide dismutase (*MnSod*), were then analysed using real-time qRT-PCR. The results are expressed as the mean ± SEM of triplicate measurements and are representative of three independent experiments. Different letters indicate statistically significant differences ($p \leq 0.05$) among the different groups.

six double bounds is highly susceptible to oxidation. In this sense, other authors have reported that DHA-enriched cells are more susceptible to oxidative insult, resulting in an exacerbation of ROS generation [34] and depending on the concentrations and conditions used, some responses could be affected, so it will be useful to protect these cells with antioxidants [35]. The main objective then is to test if EGCG, a well-known potent antioxidant, could reverse and avoid cellular oxidative damage related to DHA.

In aerobic organisms, approximately 85–90% of cellular oxygen is consumed by mitochondria to produce energy in the form of ATP molecules, concomitant with the formation of ROS. ROS induce chemical modifications in other molecules, generating oxidative damage, regulating signal transduction components, and acting as second messengers for various physiological and pathological stimuli [36]. We wanted to study the effects of DHA and EGCG at the level of mitochondrial dynamics and bioenergetics in muscle cells. Results suggest that although the DHA compound is not toxic to the cells, this compound leads to altered mitochondrial dynamics, with subsequent changes in mitochondrial function, including alteration in respiration and ROS generation.

The results from the *in vivo* oxygen consumption assay indicate that substrate oxidation was decreased in the Routine and Leak states, by the DHA and EGCG + DHA treatments. In addition, DHA-treated cells clearly consumed less oxygen during the entire recording protocol. A few studies have used dietary fish oil to investigate the influence of

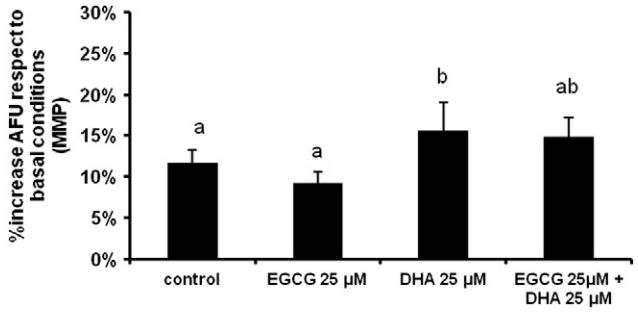

Fig. 5. Mitochondrial membrane potential in L6 cells treated with EGCG, DHA or DHA + EGCG. Cells were incubated with 25 μM epigallocatechin-3-gallate (EGCG), docosahexaenoic acid (DHA) or EGCG + DHA for 4 h. The mitochondrial membrane potential (MMP) was then measured by the addition of oligomycin to inhibit ATP production and subsequently with, carbonyl cyanide 4-(trifluoromethoxy) phenylhydrazone (FCCP) to achieve to the maximal membrane depolarization. The results are expressed as % of arbitrary fluorescence unit (AFU) increase with respect to basal conditions, compared to control treatment. Results are expressed as the mean ± SEM of triplicate measurements and are representative of three independent experiments. Different letters indicate statistically significant differences ($p \leq 0.05$) among the different groups. Arbitrary fluorescence units (AFU).

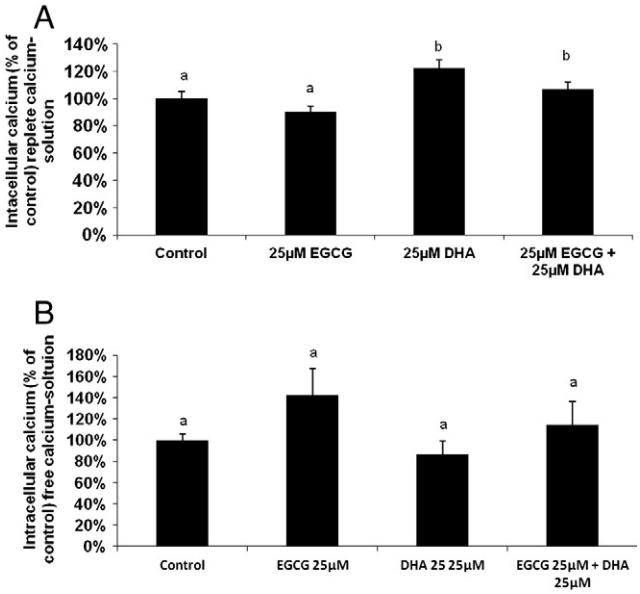

Fig. 6. Intracellular calcium levels in L6 cells treated with EGCG, DHA or DHA + EGCG. Cells were incubated with 25 μM epigallocatechin-3-gallate (EGCG), docosahexaenoic acid (DHA) or EGCG + DHA for 4 h. Intracellular calcium levels were then measured in different medium conditions: A. calcium-free medium and B. calcium-replete medium. The results are expressed as the mean ± SEM of triplicate measurements and are representative of three independent experiments. Different letters indicate statistically significant differences ($p \leq 0.05$) among the different groups.

omega-3 PUFAs on mitochondrial respiration and have reported either no change or decreases during some measurements of various substrates [19,37]. Here, with the decrease in mitochondrial respiration, mitochondrial functionality was also affected. DHA may have contributed as a potent deregulator of O_2 consumption and oxidative phosphorylation with the decreasing bioenergetic activities being, in part, due to the result of membrane perturbations caused by DHA [19].

The incubation of L6 myocytes with 25 μM DHA for 4 h led to an increase (150%) in intracellular ROS production without causing loss of cell viability. This result is in agreement with the interaction or incorporation of added DHA into the cell membrane phospholipid composition [38,39] and the susceptibility of most omega-3 PUFAs to produce oxidative damage in cells [40]. In addition, many lipid peroxidation products are themselves very potent ROS producers that can induce considerable damage to other biological molecules [37]. However oxidative stress from ROS could be a cause and a consequence of the observed mitochondrial alteration and addresses the possibility that ROS precede DHA changes in mitochondrial dysfunction. The increased ROS levels in the DHA group led to *MnSod* overexpression, which is one of the primary antioxidant responses to elevated ROS production [41,42] a part from the *Ucp3* overexpression during DHA treatment that might also

Table 2
mRNA expression for mitochondrial dynamics in L6 cells treated with DHA, EGCG or DHA + EGCG.

	Control	EGCG (25 μM)	DHA (25 μM)	EGCG + DHA (25 μM each)
Fiss1	1.00 ± 0.01a	0.96 ± 0.04a	0.67 ± 0.04b	0.71 ± 0.04b
Drp1	1.00 ± 0.03a	0.90 ± 0.05ab	0.77 ± 0.0b	0.72 ± 0.02b
Mfn2	1.00 ± 0.03a	0.92 ± 0.01a	0.76 ± 0.01b	0.85 ± 0.05ab
Opa1	1.01 ± 0.05a	1.05 ± 0.05a	0.93 ± 0.08a	0.90 ± 0.04a

Cells were incubated with 25 μM epigallocatechin-3-gallate (EGCG), docosahexaenoic acid (DHA) or EGCG + DHA for 4 h to analyse using real-time qRT-PCR different mRNA levels associated with the mitochondrial dynamics system, such as mitochondrial fission 1 protein (*Fiss1*), dynamin related protein 1 (*Drp1*), mitofusin 2 (*Mfn2*), and optic atrophy 1 (*Opa1*). The results are expressed as the mean ± SEM of triplicate measurements and are representative of three independent experiments. Different letters indicate statistically significant differences ($p \leq 0.05$) among the different groups.

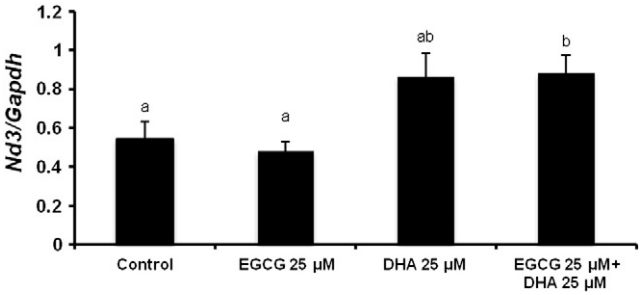

Fig. 7. mtDNA/nDNA of L6 cells treated with EGCG, DHA or EGCG+ DHA. Cells were incubated with 25 μM epigallocatechin-3-gallate (EGCG), docosahexaenoic acid (DHA) or EGCG + DHA for 4 h. mtDNA/nDNA ratio was expressed as the Nd3/GAPDH ratio by real time PCR. NADH-dehydrogenase subunit 3 (Nd3) as mitochondrial DNA and glyceraldehydes-3-phosphate dehydrogenase (*Gapdh*) as nuclear DNA. The results are expressed as the mean ± SEM of triplicate measurements and are representative of three independent experiments. Different letters indicate statistically significant differences ($p \leq 0.05$) among the different groups.

protect myocytes from ROS already described in mouse myotubes under oxidative stress conditions [43]. Moreover the DHA cell treatment increased ADP/ATP ratio with a downregulation of *Ant1* gene expression, which blocked the exchange of ADP and ATP across the mitochondrial inner membrane and disrupted the energy homeostasis, concomitant with lowered mitochondrial functionality through ETC and oxidative phosphorylation (OXPHOS) system disruptions, with *Cox* gene downregulation and the decrease of the oxygen consumption with low respiratory capacity with the incapacity to increase respiration upon the addition of FCCP shown in the DHA treatment, as other authors have reported [44–46]. The impairment in mitochondrial functionality was reversed in the EGCG + DHA group, whereas the ROS levels remained at the same levels as the control cells, which is consistent with the role of EGCG as a potent antioxidant [47] and as an uncoupler-like [48] compound, decreasing ROS production. The polyphenol structure of EGCG facilitates its capacity to penetrate membranes, resulting in ROS scavenging between the mitochondrial membrane and matrix [49]. It is important to emphasise that the overexpression of *Ucp2* and *Ucp3* was maintained in the DHA + EGCG group because, despite the antioxidant effects of EGCG, DHA was still present in the culture media.

Furthermore, mitochondria also participate in intracellular Ca^{2+} homeostasis *via* several Ca^{2+} uptake and release pathways, and ROS production could affect Ca^{2+} homeostasis due to the deterioration of membranes that contain the intracellular Ca^{2+} stores [50,51]. The

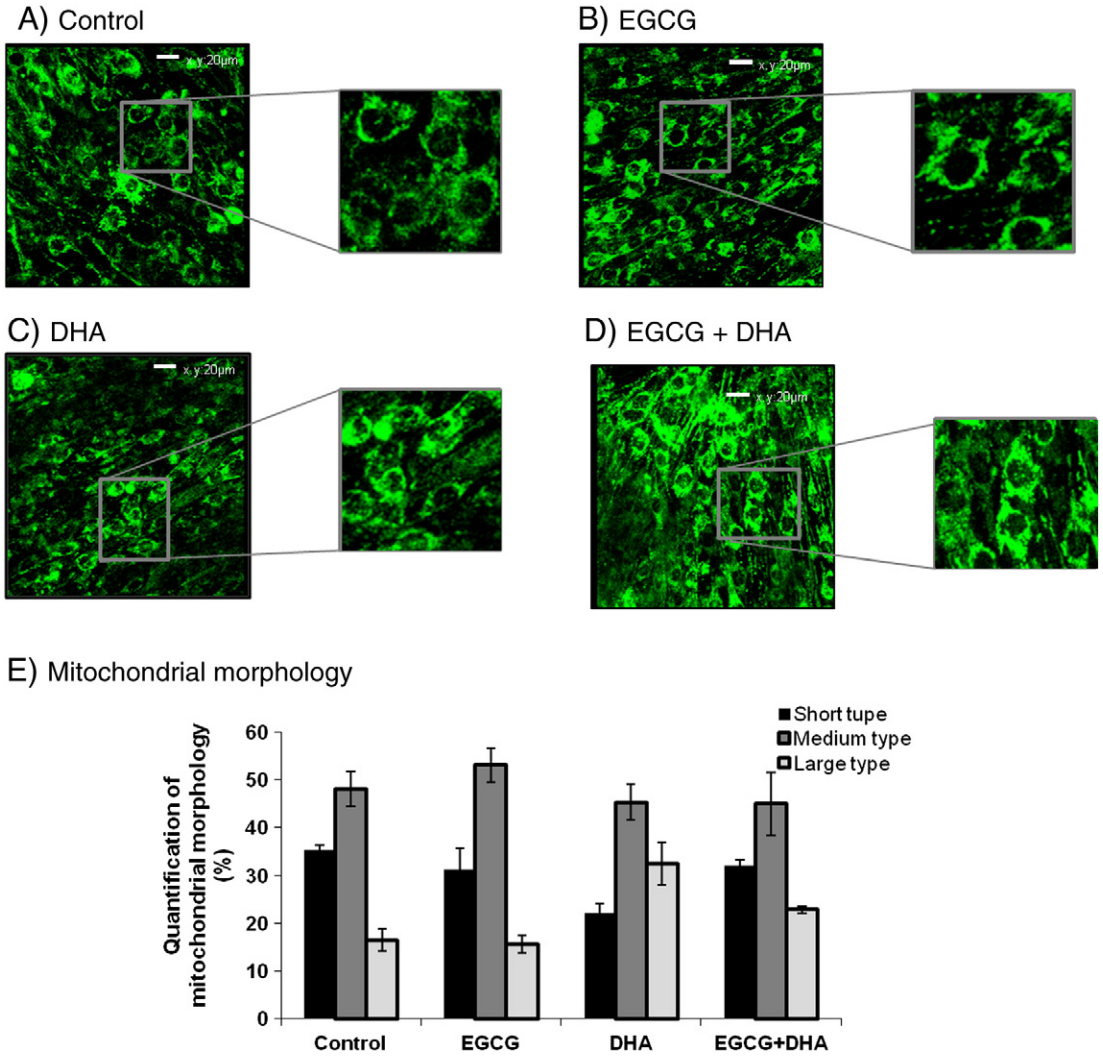

Fig. 8. Mitochondrial morphology of L6 cells treated with EGCG, DHA or DHA + EGCG. Cells were incubated with 25 μM epigallocatechin-3-gallate (EGCG), docosahexaenoic acid (DHA) or EGCG + DHA for 4 h. The mitochondrial network and morphology were visualised using MitoTracker Green FM staining and a confocal microscope. A. Control, B. EGCG 25 μM, C. DHA 25 μM and D. EGCG + DHA (25 μM each). E. Mitochondria morphology quantification (%). For the quantification of mitochondrial morphology, mitochondrial length was measured and grouped into three categories as follows: short type (1 μm ≤ in length), medium rod type (1–2 μm in length) and long type (>2 μm) using Image J software. Results are shown as a percentage of the total number of mitochondria counted per treatment.

results from the present study reveal that the DHA treated cells displayed higher intracellular Ca^{2+} levels when Ca^{2+} was supplemented in the culture media. Accordingly, it appears that the high levels of ROS produced by DHA membrane incorporation or through alterations of the cell membrane phospholipid composition induced a calcium influx of external calcium that was not from mitochondria or other calcium stores.

Mitochondrial metabolic changes could be produced by the variation in membrane fatty acid composition that is linked with the respiratory activity and OXPHOS functionality, so the downregulation of fission (*Fiss1*, *Drp1*) and fusion (*Mfn2*) gene expression during DHA treatment is a mechanism to compensate mitochondrial function and to restore mitochondrial tubules [8] maintaining freedom for both fusion and fission that is a fundamental factor to ensure adequate bioenergetics utility of the mitochondria.

Another compensatory mechanism is the higher mtDNA/nDNA ratio of the DHA-treated cells, suggesting that endogenous and exogenous oxidative stresses are factors involved in the increase of the mitochondrial abundance and mtDNA copy number in human and animal cells [3], resulting from a feedback response that compensates for defective mitochondria, hallmarks of an impaired respiratory chain or mutated mtDNA [52]. The *Fiss1* and *Drp1* gene expression were also downregulated with more rounded and elongated, short and medium length mitochondria developing functional machineries and restoring mitochondrial tubules [4,53,54] in the EGCG + DHA group. This inhibition of fission events could also repair mitochondrial damage that allows the mixing of mtDNA from other mitochondria becoming more elongated. Moreover endogenous respiration in the Routine state was also low concomitantly with altered mitochondrial morphology and cellular bioenergetic dynamics as other authors had reported [55–57], and similar to the DHA group, due to the PUFA-containing mitochondrial membranes [46] which leads to oxidative damage. In addition, it has previously been demonstrated that *Drp1* downregulation in HeLa cells leads to slower cell growth, ETC uncoupling, decreased cellular respiration and increased ROS levels [55], as what occurred here in L6 myocytes after DHA treatment. Mitochondrial morphology images reveal that in DHA treatment the majority of the mitochondria were large, elongated with some fragmented compared to control cells, as described in 3T3-L1 adipocyte studies [58,59] and could be caused by the downregulation of *Fiss1* and *Drp1* gene expression as described in rat skeletal muscle studies [60]. In addition, this deregulated mitochondrial morphology might lead to alterations in oxidative phosphorylation [8,61] as we had been shown in cells treated with DHA, although the imbalance in mitochondrial architecture in this situation revealed that mitochondria are able to adjust their own metabolism, to keep the cell alive; that is what we call adaptive response to understand mitochondrial physiology. The data presented fit our hypothesis indicating that the antioxidant and uncoupling abilities of EGCG mentioned above, influence mitochondrial morphology, reduce DHA intracellular ROS overproduction, and alter the ADP/ATP ratio and expression of *Cox* and *Ant1* genes to control levels.

In conclusion, the combination of DHA + EGCG could be a good choice for avoiding and correcting the possible deleterious effects of DHA.

Acknowledgements

This work was supported by grant number AGL 2008-00387/ALI from the Spanish Government.

References

[1] T. Tatsuta, T. Langer, Quality control of mitochondria: protection against neurodegeneration and ageing, EMBO J. 27 (2008) 306–314.
[2] H.C. Lee, Y.H. Wei, Mitochondrial role in life and death of the cell, J. Biomed. Sci. 7 (2000) 2–15.
[3] H.C. Lee, Y.H. Wei, Mitochondrial biogenesis and mitochondrial DNA maintenance of mammalian cells under oxidative stress, Int. J. Biochem. Cell Biol. 37 (2005) 822–834.
[4] X. Fan, R. Hussien, G.A. Brooks, H_2O_2-induced mitochondrial fragmentation in C_2C_{12} myocytes, Free Radic. Biol. Med. 49 (2010) 1646–1654.
[5] M. Smith, T. Tippetts, E. Brassfiled, B. Tucker, A. Ockey, A. Swensen, T. Anthonymuthu, T. Washburn, D. Kane, J. Prince, B. Bikman, Mitochondrial fission mediates ceramide-induced metabolic disruption in skeletal muscle, Biochem. J. (2013), http://dx.doi.org/10.1042/BJ20130807.
[6] H. Jheng, P. Tsai, S. Guo, L. Kuo, C.S. Chang, I. Su, C. Chang, Y. Tsai, Mitochondrial fission contributes to mitochondrial dysfunction and insulin resistance in skeletal muscle, Mol. Cell. Biol. 32 (2011) 309–319.
[7] D. Bach, S. Pich, F.X. Soriano, N. Vega, B. Baumgartner, J. Oriola, J.J. Daugaard, J. Lloberas, M. Camps, J.R. Zierath, R. Rabasa-Lhoret, H. Wallber-Henriksson, M. Laville, M. Palacin, H. Vidal, F. Rivera, F. Brand, A. Zorzano, Mitofusin-2 determines mitochondrial network architecture and mitochondrial metabolism, J. Biol. Chem. 278 (2003) 17190–17197.
[8] Y. Zhang, L. Jiang, W. Hu, Q. Zheng, W. Ziang, Mitochondrial dysfunction during in vitro hepatocyte steatosis is reversed by omega-3 fatty acid-induced up-regulation of mitofusin 2, Metab. Clin. Exp. 60 (2011) 767–775.
[9] W. Stanley, R.J. Khairallah, E.R. Dabkowski, Update on lipids and mitochondrial function: impact of dietary n − 3 polyunsaturated fatty acids, Curr. Opin. Clin. Nutr. Metab. Care 15 (2012) 122–126.
[10] A. Briolay, R. Jaafar, G. Nemoz, L. Bessueille, Myogenic differentiation and lipid–raft composition of L6 skeletal muscle cells are modulated by PUFAs, Biochim. Biophys. Acta Biomembr. 1828 (2013) 602–613.
[11] K.D. Stark, S. Lim, N. Salem, Docosahexaenoic acid and n − 6 docosapentaenoic acid supplementation alter rat skeletal muscle fatty acid composition, Lipids Health Dis. 6 (2007).
[12] S.K. Abbott, P.L. Else, A.J. Hulbert, Membrane fatty acid composition of rat skeletal muscle is most responsive to the balance of dietary *n* − 3 and *n* − 6 PUFA, Br. J. Nutr. 103 (2010) 522.
[13] G. Schmitz, J. Ecker, The opposing effects of n − 3 and n − 6 fatty acids, Prog. Lipid Res. 47 (2008) 147–155.
[14] S.R. Wassall, W. Stillwell, Polyunsaturated fatty acid–cholesterol interactions: domain formation in membranes, Biochim. Biophys. Acta Biomembr. 1788 (2009) 24–32.
[15] L.A. Witting, C.C. Harvey, B. Century, M.K. Horwitt, Dietary alterations of fatty acids of erythrocytes and mitochondria of brain and liver, J. Lipid Res. 2 (1961) 412–418.
[16] S. Tsalouhidou, C. Argyrou, G. Theofilidis, D. Karaoglanidis, E. Orfanidou, M.G. Nikolaidis, A. Petridou, V. Mougios, Mitochondrial phospholipids of rat skeletal muscle are less polyunsaturated than whole tissue phospholipids: implications for protection against oxidative stress, J. Anim. Sci. 84 (2006) 2818–2825.
[17] S. Rohrbach, Effects of dietary polyunsaturated fatty acids on mitochondria, Curr. Pharm. Des. 15 (2009) 4103–4116.
[18] N. Salem, H. Kim, J. Yergey, Docosahexaenoic acid: membrane function and metabolism, in: A.P. Simopoulos, R.R. Kifer, R.E. Martin (Eds.), Health Effects of Polyunsaturated Fatty Acids in Seafoods, Academic Press, 1986, pp. 263–317.
[19] W. Stillwell, L. Jenski, F. Crump, W. Ehringer, Effect of docosahexaenoic acid on mouse mitochondrial membrane properties, Lipids 32 (1994) 497–506.
[20] S. Liu, V.E. Baracos, H.A. Quinney, M.T. Clandinin, Dietary omega-3 and polyunsaturated fatty acids modify fatty acyl composition and insulin binding in skeletal-muscle sarcolemma, Biochem. J. 299 (1994) 831–837.
[21] A.T. Quintanilha, L. Packer, J.M.S. Davies, T.L. Racanelli, K.J.A. Davies, Membrane effects of vitamin E deficiency: bioenergetic and surface charge density studies of skeletal muscle and liver mitochondria, Ann. N. Y. Acad. Sci. 393 (1982) 32–47.
[22] D. Dorta, A. Acácio, F.E. Mingatto, T. Rodrigues, C.R. Pestana, S.A. Uyemura, A.C. Santos, C. Curtil, Antioxidant activity of flavonoids in isolated mitochondria, Phytother. Res. 22 (2008) 1213–1218.
[23] Y. Wang, U. Bachrach, The specific anti-cancer activity of green tea (−)-epigallocatechin-3-gallate (EGCG), Amino Acids 22 (2002) 131–143.
[24] M. Hiroyasu Iso, P. Chigusa Date, M. Kenji Wakai, P. Mitsuru Fukui, M. Akiko Tamakoshi, The relationship between green tea and total caffeine intake and risk for self-reported Type 2 diabetes among Japanese adults, Ann. Intern. Med. 144 (2006).
[25] B.N. Singh, S. Shankar, R.K. Srivastava, Green tea catechin, epigallocatechin-3-gallate (EGCG): mechanisms, perspectives and clinical applications, Biochem. Pharmacol. 82 (2011) 1807–1821.
[26] J.D. Lambert, R.J. Elias, The antioxidant and pro-oxidant activities of green tea polyphenols: a role in cancer prevention, Arch. Biochem. Biophys. 501 (2010) 65–72.
[27] J.P. Robinson, L.H. Bruner, C.F. Bassoe, J.L. Hudson, P.A. Ward, S.H. Phan, Measurement of intracellular fluorescence of human monocytes relative to oxidative metabolism, J. Leukocyte Biol. 43 (1988) 304–310.
[28] A. Zorzano, M.I. Hernández-Alvarez, M. Palacín, G. Mingrone, Alterations in the mitochondrial regulatory pathways constituted by the nuclear co-factors PGC-1α or PGC-1β and mitofusin 2 in skeletal muscle in type 2 diabetes, Biochim. Biophys. Acta Bioenerg. 1797 (2010) 1028–1033.
[29] P.M. Kris-Etherton, W.S. Harris, L.J. Appel, for the Nutrition Committee, Fish consumption, fish oil, Omega-3 fatty acids, and cardiovascular disease, Circulation 106 (2002) 2747–2757.
[30] C.J. Lavie, R.V. Milani, M.R. Mehra, H.O. Ventura, Omega-3 polyunsaturated fatty acids and cardiovascular diseases, J. Am. Coll. Cardiol. 54 (2009) 585–594.
[31] J. Liu, W. Shen, B. Zhao, Y. Wang, K. Wertz, P. Webber, P. Zhang, Targeting mitochondrial biogenesis for preventing and treating insulin resistance in diabetes

and obesity: hope from natural mitochondrial nutrients, Adv. Drug Deliv. Rev. 61 (2009) 1343–1352.
[32] R. Rastmanesh, High polyphenol, low probiotic diet for weight loss because of intestinal microbiota interaction, Chem. Biol. Interact. 15 (2011) 1–8.
[33] W. Stillwell, S.R. Wassall, Docosahexaenoic acid: membrane properties of a unique fatty acid, Chem. Phys. Lipids 126 (2003) 1–27.
[34] A. Fernández-Iglesias, H. Quesada, S. Díaz, D. Pajuelo, C. Bladé, L. Arola, M. Josepa Salvadó, M. Mulero, DHA sensitizes FaO cells to tert-BHP-induced oxidative effects. Protective role of EGCG, Food Chem. Toxicol. 62 (2013) 750–757.
[35] W. Stillwell, The role of polyunsaturated lipids in membrane raft function, Scand. J. Food Nutr. 50 (2006) 1007–1113.
[36] R. Foncea, C. Carvajal, C. Almarza, F. Leighton, Endothelial cell oxidative stress and signal transduction, Biol. Res. 33 (2000) 86–96.
[37] S. Yamaoka, R. Urade, M. Kito, Mitochondrial function in rats is affected by modification of membrane phospholipids with dietary sardine oil, J. Nutr. 118 (1988) 290–296.
[38] M.Y. Hong, R.S. Chapkin, R. Barhoumi, R.C. Burghardt, N.D. Turner, C.E. Henderson, L.M. Sanders, Y. Fan, L.A. Davidson, M.E. Murphy, C.M. Spinka, R.J. Carroll, J.R. Lupton, Fish oil increases mitochondrial phospholipid unsaturation, upregulating reactive oxygen species and apoptosis in rat colonocytes, Carcinogenesis 23 (2002) 1919–1926.
[39] S.M. Watkins, L.C. Carter, J.B. German, Docosahexaenoic acid accumulates in cardiolipin and enhances HT-29 cell oxidant production, J. Lipid Res. 39 (1998) 1583–1588.
[40] R. Pamplona, D. Costantini, Molecular and structural antioxidant defenses against oxidative stress in animals, Am. J. Physiol. Regul. Integr. Comp. Physiol. 301 (2011) R843–R863.
[41] A.E. Civitarese, P.S. MacLean, S. Carling, L. Kerr-Bayles, R.P. McMillan, A. Pierce, T.C. Becker, C. Moro, J. Finlayson, N. Lefort, C.B. Newgard, L. Mandarino, W. Cefalu, K. Walder, G.R. Collier, M.W. Hulver, S.R. Smith, E. Ravussin, Regulation of skeletal muscle oxidative capacity and insulin signaling by the mitochondrial rhomboid protease PARL, Cell Metab. 11 (2010) 412–426.
[42] L.A. Esposito, S. Melov, A. Panov, B.A. Cottrell, D.C. Wallace, Mitochondrial disease in mouse results in increased oxidative stress, Proc. Natl. Acad. Sci. U. S. A. 96 (1999) 4820–4825.
[43] E. Barreiro, C. Garcia-Martínez, S. Mas, E. Ametller, J. Gea, J.M. Argilés, S. Busquets, F.J. López-Soriano, UCP3 overexpression neutralizes oxidative stress rather than nitrosative stress in mouse myotubes, FEBS Lett. 583 (2009) 350–356.
[44] H. Chen, A. Chomyn, D.C. Chan, Disruption of fusion results in mitochondrial heterogeneity and dysfunction, J. Biol. Chem. 280 (2005) 26185–26192.
[45] A.E. Civitarese, E. Ravussin, Minireview: mitochondrial energetics and insulin resistance, Endocrinology 149 (2008) 950–954.
[46] P. Marchetti, M. Castedo, S. Susin, H. Zamzami, N.T.A. Macho, A. Haeffner, F. Hirsch, M. Geuskens, G. Kroemer, Mitochondrial permeability transition is a central coordinating event of apoptosis, J. Exp. Med. 184 (1996) 1155–1160.
[47] J. Franco, H. Braga, J. Stringari, F.C. Missau, T. Posser, B.G. Mendes, R.B. Leal, A.S. Santos, A. Dabre, M.G. Pizzolatti, M. Farina, Mercuri-induced hydrogen peroxide generation in mouse brain mitochondria: protective effects of quercetin, Chem. Res. Toxicol. 20 (2007) 1919–1926.
[48] M. Modrianský, E. Gabrielová, Uncouple my heart: the benefits of inefficiency, J. Bioenerg. Biomembr. 41 (2009) 133–136.
[49] S. Wolfram, Effects of green tea and EGCG on cardiovascular and metabolic health, J. Am. Coll. Nutr. 26 (2007) 373S–388S.
[50] M.T. Lin, M.F. Beal, Mitochondrial dysfunction and oxidative stress in neurodegenerative diseases, Nature 443 (2006) 787–795.
[51] C. Giorgi, C. Agnoletto, A. Bononi, M. Bonora, E. De Marchi, S. Marchi, S. Missiroli, S. Patergnani, F. Poletti, A. Rimessi, J.M. Suski, M.R. Wieckowski, P. Pinton, Mitochondrial calcium homeostasis as potential target for mitochondrial medicine, Mitochondrion 12 (2012) 77–85.
[52] A. Barrientos, J. Casademont, F. Cardellach, E. Ardite, X. Estivill, A. Urbano-Márquez, J.C. Fernández-Checa, V. Nunes, Qualitative and quantitative changes in skeletal muscle mtDNA and expression of mitochondrial-encoded genes in the human aging process, Biochem. Mol. Med. 62 (1997) 165–171.
[53] N. Mishra, R. Kar, P.K. Singha, M.A. Venkatachalam, D.G. McEwen, P. Saikumar, Inhibition of mitochondrial division through covalent modification of Drp1 protein by 15 deoxy-Δ12,14-prostaglandin J2, Biochem. Biophys. Res. Commun. 395 (2010) 17–24.
[54] H. Chen, D.C. Chan, Mitochondrial dynamics in mammals, Curr. Top. Dev. Biol. 59 (2004) 119–144.
[55] H. Bo, Y. Zhang, L.L. Ji, Redefining the role of mitochondria in exercise: a dynamic remodeling, Ann. N. Y. Acad. Sci. 1201 (2010) 121–128.
[56] A. Zorzano, M. Liesa, M. Palacín, Mitochondrial dynamics as a bridge between mitochondrial dysfunction and insulin resistance, Arch. Physiol. Biochem. 115 (2009) 1–12.
[57] S. Pich, D. Bach, P. Briones, M. Liesa, M. Camps, X. Testar, M. Palacín, A. Zorzano, The Charcot–Marie–Tooth type 2A gene product, Mfn2, up-regulates fuel oxidation through expression of OXPHOS system, Hum. Mol. Genet. 14 (2005) 1405–1415.
[58] T. Kita, H. Nishida, H. Shibata, S. Niimi, T. Higuti, N. Arakaki, Possible role of mitochondrial remodeling on cellular triacylglycerol accumulation, J. Biochem. 146 (2009) 787–796.
[59] S.M. Horner, H.M. Liu, H.S. Park, J. Briley, M. Gale, Mitochondrial-associated endoplasmic reticulum membranes (MAM) form innate immune synapses and are targeted by hepatitis C virus, Proc. Natl. Acad. Sci. 108 (2011) 14590–14595.
[60] H. Ding, N. Jiang, H. Liu, X. Liu, D. Liu, F. Zhao, L. Wen, S. Liu, L.L. Ji, Y. Zhang, Response of mitochondrial fusion and fission protein gene expression to exercise in rat skeletal muscle, Biochim. Biophys. Acta Gen. Subj. 1800 (2010) 250–256.
[61] A.S. Rambold, B. Kostelecky, N. Elia, J. Lippincott-Schwartz, Tubular network formation protects mitochondria from autophagosomal degradation during nutrient starvation, Proc. Natl. Acad. Sci. 108 (2011) 10190–10195.